Short Paper: Microgrid Losses - When the Whole is Greater Than the Sum of Its Parts

Maxim Buevich † Xiao Zhang † Dan Schnitzer ‡ Tristan Escalada ‡
Arthur Jacquiau-Chamski ‡ Jon Thacker ‡ Anthony Rowe †
† Electrical and Computer Engineering Department, Carnegie Mellon University
‡ SparkMeter Inc.
{mbuevich,xiaozhan,agr}@andrew.cmu.edu
{dan,tristan,arthur,jon}@sparkmeter.io

ABSTRACT

Non-Technical Loss (NTL) represents a major challenge when providing reliable electrical service in developing countries, where it often accounts for 11-15% of total generation capacity [1]. NTL is caused by a variety of factors such as theft, unmetered homes, and inability to pay which at volume can lead to system instability, grid failure, and major financial losses for providers.

In this paper, we investigate error sources and techniques for separating NTL from total losses in microgrids. Our approach models the primary sources of state uncertainty including line losses, transformer losses, meter calibration error, packet loss, and sample synchronization error. We conduct an extensive data-driven simulation on 72 days of wireless meter data from a 430-home microgrid deployed in Les Anglais, Haiti. We show that the model can be used to determine uncertainty bounds that can help in separating NTL from total losses.

Keywords

Microgrid, NTL Detection

1. INTRODUCTION

As reported by the World Bank Group in 2011 [1], Non-Technical Loss (NTL) accounts for 15% of total generation capacity in the Latin America & Caribbean market and 11% in the Sub-Saharan Africa markets. Together with corruption and weak regulatory environments, NTL are a major contributor to the poor state of operations of utilities in developing countries [2]. NTL prevents utilities from achieving cost recovery because they cannot fully pay for the cost of energy generated. This leads to a vicious cycle: inability to pay for generation results in supply shortages that cause outages; outages result in customer dissatisfaction, so even customers who were paying for electricity may be less inclined to do so and may self-generate rather than purchase electricity from the utility; a smaller customer base results in even lower tariff collection, and then even greater supply shortages.

Utilities would benefit greatly from being able to locate NTL and address the problem with consumers directly. Smart metering enables utilities to do this on a real-time basis, whereas conventional metering systems provide utilities with only a monthly resolution.

Theft is a large component of NTL on both central and remote microgrids [3]. Most often, theft is carried out by making an unauthorized connection to the microgrid distribution line. In other cases, theft is carried out by authorized customers who bypass their meters. Monitoring theft is therefore difficult, especially on systems that serve a few hundred households. Theft is most often dealt with through strong local institutions that can impose a credible threat of penalty. However, penalties are often unenforced, and theft persists on many systems due to lack of visibility into losses.

In this paper, we discuss the detection of NTL in a rural microgrid deployment in Les Anglais (LA), Haiti. An initial version of the microgrid was first described in [4] which included wireless energy meters on 54 homes. The system utilized excess capacity from a diesel generator powering a local cellular tower. Over the last year, we have updated the microgrid with a commercial version of the system developed by SparkMeter Inc. The grid now services more than 430 homes powered by a 93kW solar PV array with 400kWh of battery capacity and an auxiliary diesel backup generator. We use detailed characteristics of the distribution network, communication network and data traces collected from the microgrid to drive our NTL simulations.

One of the novel features of our underlying system is the use of time synchronized sampling of power data across the network to aid in separating NTL from total losses. We determine the state of the microgrid system by comparing all of our meter readings with a set of totalizers installed at each generation source. Ideally, the sum of the loads should match the generation. However, there are multiple sources of error including (1) line losses (and transformer losses), (2) metering error, (3) packet loss and (4) temporal meter sampling jitter. We define this difference as the grid's *State Error*. Using a trace-driven simulation of our network, we explore the magnitude and implications of each of these sources of error. We show how the combination of modeling and synchronous sampling can yield action-able suggestions about when theft occurs and how much energy is missing.

BuildSys'15, November 04–05, 2015, Seoul, Republic of Korea
© 2015 ACM. ISBN 978-1-4503-3981-0/15/11 ...$15.00.
DOI: http://dx.doi.org/10.1145/2821650.2821676.

2. RELATED WORK

Microgrids can be an effective means to provide access to electricity in areas of the world where it is financially, physically, or institutionally difficult to extend the reach of the central grid [3]. They are developed by government agencies, private developers and NGOs around the world.

Unfortunately, many microgrids fall into non-functioning states due to any one of a number of factors, including low levels of tariff collection, poor maintenance, customer overusage (which causes brownouts), and unmet growth in demand [3]. In recent years, attempts at modeling microgrid operations have shown that a number of interventions can improve microgrid sustainability, such as the use of renewable energy to improve cost-effectiveness [5] [6] [7], energy efficiency [7], and the use of demand side management (DSM) strategies and technologies [8] [9]. In this paper, we look holistically at separation of NTL from total losses given a model of the grid, its metering characteristics, and the communication network used to collect data.

3. GRID MODEL

We perform our experiments using data collected over a 72-day period of time from the LA microgrid deployment. All of the meter readings are synchronized and accompanied by logs of wireless communication traffic along with a detailed description of the physical grid topology. In the first stage of the LA microgrid deployment, there was a period of a few weeks when data from 48 houses was being collected at 1Hz. We use this high-speed data to extrapolate what would happen as the jitter in sensor sampling increased. The full network reports data from 430 homes every 15 minutes with each meter sampling globally within approximately 10 milliseconds. Figure 1 shows an example of the power consumed over time of one home as well as the entire grid.

We employ GridLAB-D as the engine to calculate the power flow as well as our line loss statistics, using the topology of the LA grid (i.e. how the houses, power lines, service drops are connected to one another) as an input. The power line traces are captured from an annotated satellite photo; the wire properties are derived from the vendor data sheets; the pole locations are obtained from the project records; the house locations are imported from the GPS log. Our model assumes that houses are connected to the nearest utility pole. While this not true for every house on the physical grid, it is an adequate approximation for the purpose of simulation. With this topology information, as well as the synchronized measurement at each timestamp, we are able to generate a GridLAB-D input file (.glm) that models the

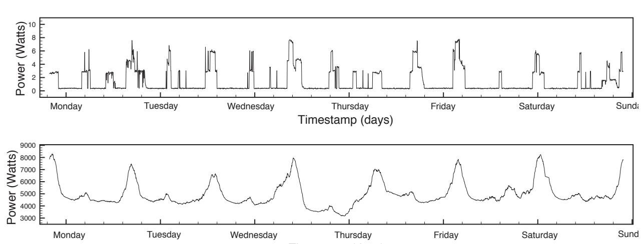

Figure 1: Example power trace over a week for a single house (top) and entire grid (bottom)

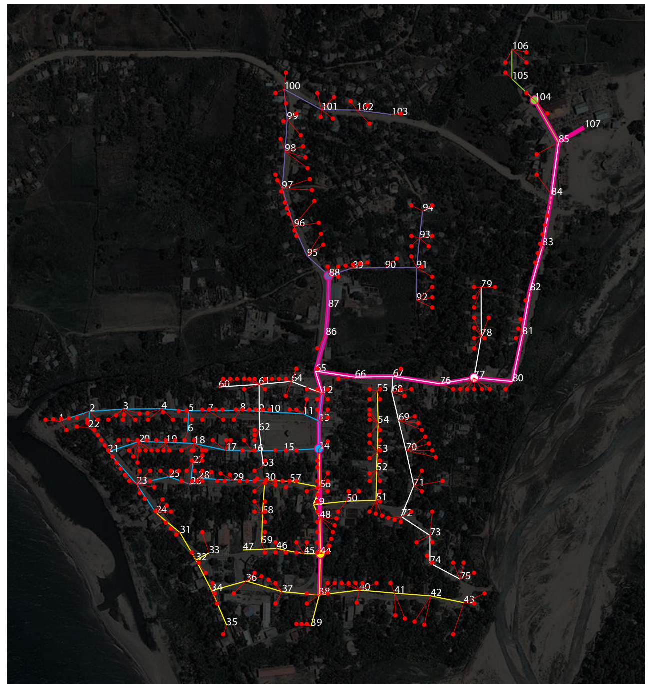

Figure 2: Les Anglais grid topology

instantaneous LA power grid. Next, GridLAB-D calculates the power flow for that timestamp and saves the results into an XML file. Finally, the XML file is analyzed to give us the line loss summary and powerflow at each node in the grid.

The topology of the LA grid is shown in Figure 2, in which different colors represent different subdivisions: the thick (pink) lines represent the three-phase Medium Voltage (MV) lines with a nominal voltage of 7.2kV. The other subdivisions are single-phase Low Voltage (LV) lines with a nominal voltage of 120V. The LV subdivisions are connected to the MV lines via split-phase transformers and to individual houses via service drops.

3.1 Line Losses

In order to understand the impact of line loss on energy theft detection, the power flows of the LA grid are simulated under multiple loading scenarios, with the assumption of nominal line voltages. There are 1102 meters of MV wiring in the grid, however, loss in the MV lines is negligible given their low gauge and high voltage. The LV lines, having an AWG of 2 and a total combined length of 4210 meters, are the primary source of line loss. We also incorporate transformer loss into our simulations; typically, one-third of loss is found in transformers and the rest in wiring.

We simulate multiple loading scenarios while varying the number of houses connected to the grid. The first scenario represents the current LA grid, where there are 430 houses connected by 6835 meters of service drops; the second scenario restricts the number of houses connected at each pole to be smaller or equal to 3, where 272 houses are connected by 4631 meters of service drops; the last scenario is the case that each pole can only connect 1 house, where there are 104 houses and the length of service drops is 1886 meters in total.

The power flows for the scenarios described above are simulated every 15 minutes for 24 hours - there are 96 simula-

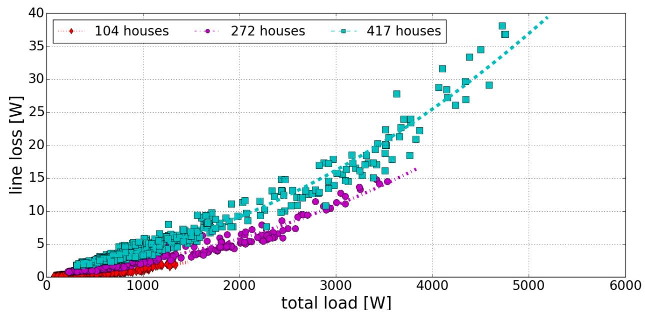

Figure 3: Simulated trace-based aggregate line loss

tions for each scenario. The line loss and the total load in the grid for each of these simulations are plotted in Figure 3, where each point stands for a simulation. From the plot, we observe that (1) the more houses connected in the grid, the higher the percentage of line loss to the total load; (2) under the same configuration, the relationship between line loss and the total load appears quadratic.

3.2 Metering Error

Metering standards like IEC 61036 specify multiple classes of meter accuracies that can range from 0.2% to 2.5% in terms of maximum error at a given power factor. After calibration, we see our meters generally exhibit Gaussian error. In the LA grid, each meter is 2.0% accurate with a typical load limit of 30 W. At maximum load each house would expect to see 0.6 W of error. Assuming a summation of Gaussian distributions, the magnitude of the noise will grow as the root mean square of the total which is relatively small even for a large number of nodes. For this reason, the aggregator's error is critical in that it will directly bound the system's ability to detect NTL.

3.3 Packet Loss

Lost meter packets play an important role in measuring the state of the system. If a meter does not report a value in a particular cycle, there are numerous error correction options including: (1) ignore the sampling period, (2) use a previous value for the dropped reading, (3) predict the value based on a model or (4) assume the worst-case consumption of the missing meter. For example, if a single meter value is missing we must increase our tolerance for detecting NTL by the expected consumption in that home during the period. Many missing meter readings compounds the problem.

In the LA microgrid, over 72 days with a 15 minute period, 94.03% of the meter polling periods returned all of the meter values. Note that the gateway continuously polls any missing meters until the start of the next period allowing for ample low-level retry opportunities (overall packet reception rate was >99.6%). Figure 4 shows the packet distributions associated with the network failure cases. The left graph shows how often consecutive periods failed to collect data from all meters. For example, there were 21 cases where the dropped data was only for a single period (15 minutes), 14 cases where it continued for two periods (30 minutes), and so on. The three large blackouts were due to scheduled grid maintenance. The right graph in Figure 4 shows the distribution of how many meters would fail to reply given a period that includes dropped messages. We see that most drops include only a few meters, but there are occasions when large areas of the network are unreachable. Given the reliability of the network and the potential for large numbers of meters to not respond, we adopt a scheme which ignores polling cycles with missing meter readings. In practice this seems sufficient, and could easily be improved with the use of previous values to replace missing data points.

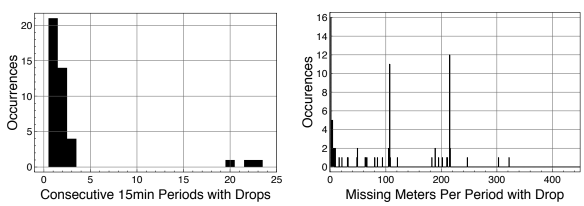

Figure 4: Network packet loss

3.4 Meter Sampling Jitter

Our method of NTL detection is fundamentally based on comparing a single sample taken by a totalizer and a summation of many distributed samples taken by wireless meters. In such a scheme, the times at which the meter samples were taken can have a significant effect on the final result. In order to understand this, we quantify the impact that this sampling jitter has on the state error calculation.

Figure 5 shows the results of a state error simulation which contains a controlled amount of sampling jitter and no other sources of error. Instead of being perfectly synchronized, meter samples are randomly selected (with a uniform distribution) from inside a synthetic jitter window, which has a width measured in seconds. As the jitter window is increased, the samples are de-synchronized. For instance, in Figure 5 we see that when sampling within a 30-second jitter window, the median state error is 0.29%; whereas, sampling within a 15-minute window, which is done by most conventional meters, results in a median state error of 1.18%.

4. NTL SIMULATION

In this section, we employ our model and collection of meter data from the Les Anglais microgrid to simulate the state error in the system. State error is observed whenever there is a mismatch between the generated power measured by the totalizer and the summation of all loads seen by the meters. Our simulator incorporates all of the primary sources of error into its calculations: line losses (0.5-1.5%), metering error (0.2-2.0%) and sampling jitter (0-2.5%). Line losses are calculated using GridLAB-D, as described in Section 3.

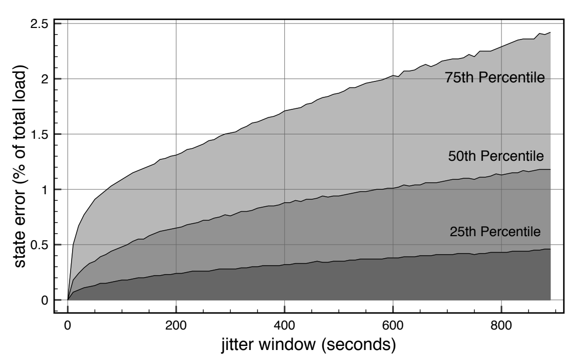

Figure 5: Impact of jitter on state error

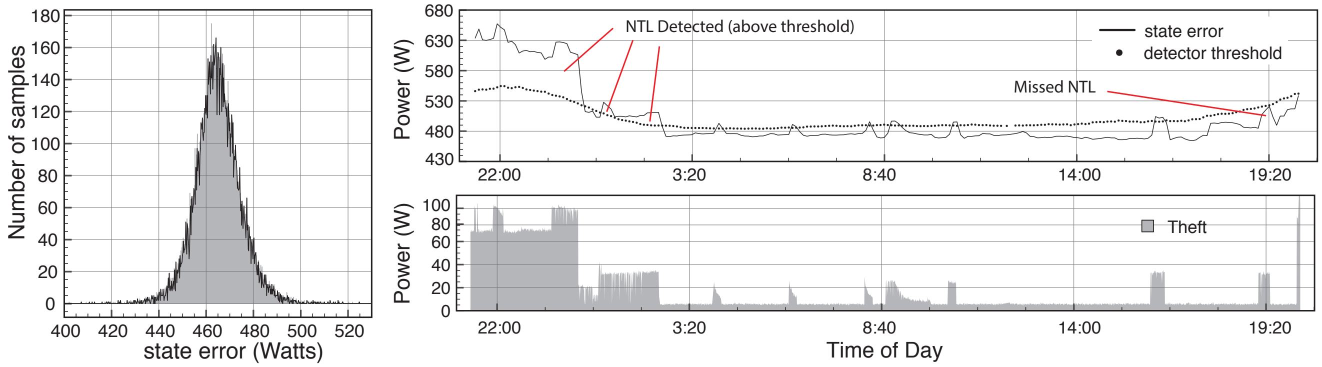

Figure 6: Distribution of state error when no NTL is present (left). NTL detector threshold as compared to state error over 24 hours (top-right) with injected NTL (bottom-right).

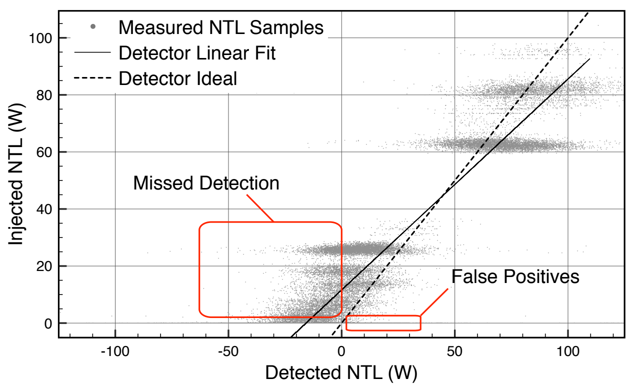

Figure 7: Performance of NTL detector

The power consumption and the sensing error of the meters were modeled as Gaussian random variables, while sampling jitter was simulated using our synthetic jitter window.

In order to illustrate the utility of approximating the sources of error, a simple proof-of-concept NTL detector was implemented on top of the simulator. The detector is based on a threshold calculated from a typical value of line loss and a small buffer. In our tests, line loss was set to 1.5% of totalizer power and the buffer was set to the 2-sigma deviation from the mean of typical state error, a distribution of which is shown in Figure 6 (left). The detector was then run against a simulation where an additional household, shown in Figure 6 (bottom-right), was injected as NTL. A detection time-series is displayed in Figure 6 (top-right), where any point at which the state error is above the threshold represents the detection of potential theft. A scatter-plot representation of detection over a week of data, seen in Figure 7, shows that the detector tends to over-estimate large quantities of NTL and cannot accurately identify NTL less than 38W. We see that the detector has a low false-positive rate of 0.2% when there is no NTL. Filtering data over time could reduce false-positives at the cost of detection latency.

5. CONCLUSIONS

In conclusion, this paper presents a case study that evaluates how modeling and synchronous sampling can be used to estimate the NTL within a microgrid. We show that line loss, sampling jitter and sensing error contribute significantly to the noise present in a metering system. We see that by modeling these sources of error we are able to reliably detect theft on the order of 0.4% (38W out of 9kW load) given our 430 home microgrid with fewer than 0.2% false positive rate. We believe that this approach will provide an extremely valuable tool for grid operators and are continuing to investigate mechanisms that learn system parameters at runtime to decrease the error detection tolerances. In the future, we intend to investigate localizing theft through multiple distributed aggregators.

6. REFERENCES

[1] World Bank Group, http://wdi.worldbank.org/table/5.11 (viewed 7/20/2015).

[2] Besant-Jones. Reforming power markets in developing countries: What have we learned. 2006.

[3] Mini-Grid Design Manual. Esmap technical paper 007. *Energy Sector Management Assistance Programme (ESMAP) UNDP/World Bank–April*, 2000.

[4] M. Buevich, D. Schnitzer, T. Escalada, A. Jacquiau-Chamski, and A. Rowe. Fine-grained remote monitoring, control and pre-paid electrical service in rural microgrids. In *Information Processing in Sensor Networks, IPSN-14 Proceedings of the 13th International Symposium on*, pages 1–11, April 2014.

[5] M. Khan and M. Iqbal. Pre-feasibility study of stand-alone hybrid energy systems for applications in newfoundland. *Renewable Energy*, 2005.

[6] Singh SP Rana S., Chandra R. and MS Sodha. Optimal mix of renewable energy resources to meet the electrical energy demand in villages of madhya pradesh. *Energy Conversion and Management*, 1998.

[7] Daniel M Kammen and Christian E Casillas. The delivery of low-cost, low-carbon rural energy services. 2011.

[8] Meg Harper. Review of strategies and technologies for demand–side management on isolated mini–grids. 2013.

[9] TG Quetchenbach, MJ Harper, J Robinson IV, KK Hervin, NA Chase, C Dorji, and AE Jacobson. The gridshare solution: a smart grid approach to improve service provision on a renewable energy mini-grid in bhutan. *Environmental Research Letters*, 8(1):014018, 2013.